

Dynamic Analysis of Rockets Launcher

Dragoljub VUJIC*, Vlado DJURKOVIC, Nikola MILENKOVIC, Slavisa TRAJKOVIC

Abstract: This paper deals with dynamic analysis of rockets launcher on a moving vehicle. Mechanical model of a launch rail system with a rocket is represented as a set of solid bodies and deformable elements with a damped elastic support. These launch rail systems enable to fire rockets of different weights and geometric configurations. Unlike them, today's multiple rocket launcher systems are located in containers. Movement of this type of mechanical system is described with three defined coordinates: movement of a rocket on a deformable ramp, curvature of the top of a deformable ramp and an angle of rotation of the ramp around its longitudinal axis. Mathematical model of the whole system, including rockets launcher and vehicle, represents a system of five nonlinear, nonhomogeneous differential equations of second order. This system is transformed to a system of 10 differential equations of the first order, suitable for numerical solving through the software package MATLAB. Rocket launcher designers can find the obtained simulation and experimental results, represented in a graphical form which is very useful during the development of a new and modification of existing constructions.

Keywords: rocket launcher; launch pad; rocket; mathematical model; dynamic model

1 INTRODUCTION

The rocket launcher belongs to a group of artillery weapons intended for attacks against enemy personnel, as well as individual fortified points deep in enemy territory. Therefore, military theorists classify it within a group of artillery weapons aimed at supporting own infantry. A rocket launcher is characterized with high firepower and maneuverability, thanks to the possibility of moving with the rockets on the launch pad. Rockets used on this type of launcher are unguided rockets. In order to achieve the necessary effect, rockets must be launched at an exactly determined angle of elevation and azimuth. As a vital part of a launcher, the launch pad has a task of holding and guiding a rocket at a desired elevation. Launch pad has to ensure with its length that it guides a rocket until a vertical component of the rocket's engine thrust vector balances the force of the rocket's weight. Dynamic parameters of a launch pad are quite broadly considered in literature. However, launch pads are considered as a solid body which does not fully correspond to real conditions in exploitation [1]. Also, in [1] author does not take elasticity of the ramp support and elasticity of the launcher support into consideration, which is quite significant having in mind that a launcher can work on the basis of different categories.

In [2] authors stated that the launcher models used in most of the previous studies had a few degrees of freedom that could not possibly capture many important motion characteristics. They used a flexible multibody model of a missile launcher system. The fixed, azimuth and elevation platforms and the launch pad were modeled as flexible bodies. The joint flexibility effects were also included to the model by spring-damper elements.

A case of a physical and mathematical model of a launcher of unguided rockets with an elastic support and solid launch pad was considered [3]. The mathematical model was classified as a coupled system with time-varying coefficients, determined, variable in time, dissipative and bounded, with five degrees of freedom.

In order to study the coupling effect of the equipment and the launching site during the erecting process of the vehicle missile system, the flexible multi-body dynamic

model is established in ADAMS [4]. The coupling calculation model of the weapon system and the launching site is established in the co-simulation of the ADAMS and MATLAB/Simulink.

In [5] authors considered the stability of launching devices during firing. They assumed that the launching device and the moving rocket form a complex oscillating system of rigid bodies bound by elastic elements (the vehicle chassis, the tilting platform and the rockets in the containers). The developed mathematical model of this oscillating system is used to determine the oscillations and their effects on the initial conditions of the rocket path.

Taking into consideration that during the firing, the rocket-launching device system oscillates and these oscillations may have a negative influence on the unguided rocket firing precision, it is necessary to evaluate the exact influence of the disturbance factors on the rocket movement upon the launcher. In [6] authors present the equations of the rocket movement upon the launcher under the disturbance factors action, taking into consideration that the rocket is the integrated part of the rocket-launching device system.

In [7] authors deal with the parameters important for defining the mechanism for elasticity elimination in the vehicle launching device. The presented basic dynamic analysis of rocket launcher is of crucial importance for discovering the influential parameters necessary for calculating the required power of the mechanism.

In [8] authors present an analysis and design of active vibration control algorithm for Multiple Launch Rocket System (MLRS). It has interesting advantages as follows: 1) Active vibration control is more competent, more pliable, and more realizable in engineering compared to passive vibration control; 2) The guidance and control package will not be destroyed. In this research, transfer matrix method of multibody system is used to build the controlled dynamic model of MLRS.

In [9] authors studied the dynamics of a vehicular missile system and determined initial disturbances of a missile. The multi-rigid-flexible launch dynamics model of a vehicular missile system was developed by using transfer matrix method for multibody system and launch dynamics theory.

Poor dispersion characteristics of rockets due to the vibration of Multiple Launch Rocket System (MLRS) have always restricted the MLRS development for several decades. Vibration control is a key technique to improve the dispersion characteristics of rockets. To approach this problem, a computed torque controller integrated with a radial basis function neural network is proposed to achieve the high-precision vibration control for MLRS [10].

In [11] authors considered the oriented control as a key technique to improve the dispersion characteristics of rockets. They proposed an orienting control method for launcher of the MLRS in a salvo firing. Because the MLRS is a typical nonlinear system, the major difficulty in designing the orienting controller lies in the nonlinearity. To deal with the nonlinearity, the concept of computed torque control is introduced.

The efficient vibration control of complex multibody systems is an important issue in engineering design and has drawn substantial attention in the field of multibody system dynamics and control engineering. In [12] authors presented an active vibration control design method for the dynamic modeling and vibration control design of multibody systems by combining the transfer matrix method for multibody systems and modal space control.

In [13] authors presented the control modeling and analysis of the prototype of Multiple Launch Rocket System (MLRS) using Matlab Simulink. The mathematical model was determined using physical law and theoretical foundation of the turning mechanism control system and the elevating mechanism control system.

In [14] authors considered a comprehensive multibody system dynamics model of a Multiple Launch Rocket System (MLRS), and its simulation and experimental studies. The new version of transfer matrix method of multibody system and the launch dynamics theory are used in deriving the equations of motion coupled with rockets and barrels.

The missile launching system is a typical complex mechanical system, which is becoming increasingly larger in scale and more complicated in structure. Designing these types of weapons often requires repeated complex and time-consuming model design, calculation, and analysis of the dynamics of the system [20]. In [15] authors put forward a new method for bidirectional-driving parameter between CAD and CAE, by changing the geometric model parameters, which directly changes the dynamics model.

The transfer matrix method for multibody systems, namely the "Rui method", is a new method for studying multibody system dynamics, which avoids the global dynamics equations of the system, keeps high computational speed, and allows highly formalized programming. Some aspects regarding the transfer matrix method for multibody systems are reviewed systematically in [16].

This paper sets and analyses a mechanical-mathematical model taking into consideration influential parameters in the rocket's launch phase. It also analyses the deformation of a launch pad, rocket's speed, influence of stiffness of the ramp support on a mechanical model with elastic support. Then, some numerical examples of a specific construction were worked out and the conclusions drawn were of interest for improving the existing or a new construction in the future.

Mechanical model of a launcher while launching a rocket (Fig. 1) was greatly based on mechanical models of analogue objects: auto-cranes and telescopic crane shafts [17]. The model consists of solid bodies and deformable elements with elastic connections. The lower part of the launcher (Fig. 1, position 1), consists of a chassis, cabin, power train aggregates and supports (tires and stabilizers). Chassis with aggregates and its corresponding elements will be considered as a solid plate supported on corresponding springs. This approximation is allowed, especially in structurally reinforced chassis. Stiffness of these springs corresponds to reduced stiffness of supports and substrate.

2 MECHANICAL-MATHEMATICAL MODEL

The upper part of the launcher (Fig. 1, position 2) including a mount, radial-axial bearing, mechanisms for raising and rotating a ramp, is considered as a solid body supported on the chassis. The launch pad (Fig. 1, position 3) represents a beam bracket (a smaller beam bracket is neglected) that is elastic and deformable in the vertical and horizontal axis (Fig. 2). The rocket (Fig. 1, position 4) represents a stiff body with a mass m .

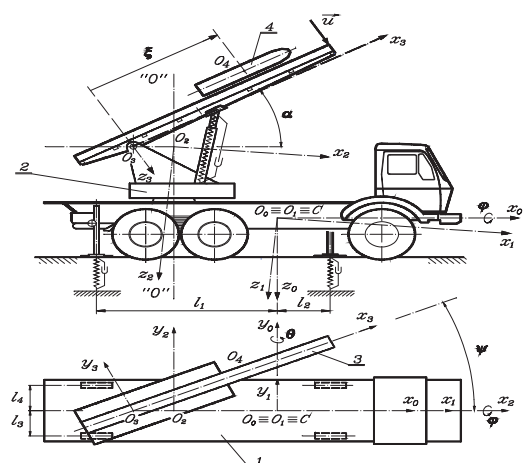


Figure 1 Mechanical launcher model

2.1 Generalized Coordinates

Movement of the presented mechanical system is defined with the following generalized coordinates (Fig. 1, Fig. 2, Fig. 3): Z_C , φ , θ , ξ , u .

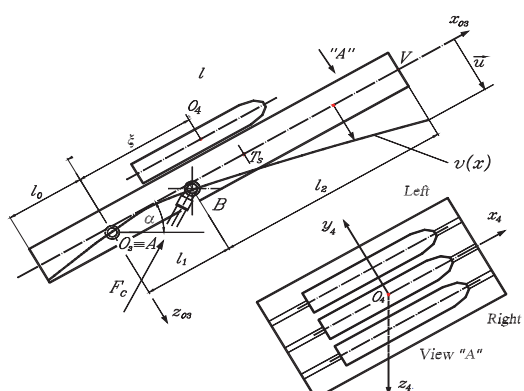


Figure 2 Launching pad with rockets

2.2 Coordinate Systems

Movement of such complex mechanical system that is considered here, was interpreted in [17], in detail. In this case, the movement is observed with respect to the following coordinate systems Fig. 1, Fig. 3): $x_0y_0z_0$, $x_1y_1z_1$, $x_2y_2z_2$, $x_3y_3z_3$. It is necessary that points C , O_1 and O_2 , coincide when the mechanical system is at rest.

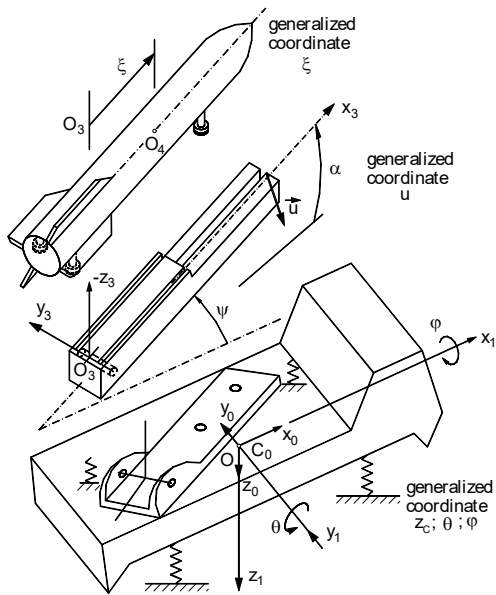


Figure 3 Generalized coordinates of the mechanical system

2.3 Coordinate Systems

Kinetic energy of the system is:

$$E_k = E_{k1} + E_{k2} \quad (1)$$

where:

$$\begin{aligned} E_{k1} &= \frac{1}{2} m_1 v_1^2 + \frac{1}{2} J_{l_1} \dot{\phi}_1^2 + \frac{1}{2} J_{l_1} \dot{\theta}_1^2 + \frac{1}{2} m_L v_L^2 + \frac{1}{2} J_{L_2} \dot{\phi}_2^2 + \frac{1}{2} J_{L_2} \dot{\theta}_2^2 \\ E_{k2} &= \frac{1}{2} m_r v_r^2 + \frac{1}{2} J_{r_y} \dot{\phi}_r^2 + \frac{1}{2} m_s v_s^2 + \frac{1}{2} J_{s_y} \dot{\phi}_s^2 + \frac{1}{2} J_{r_y} \dot{\theta}_r^2 + \frac{1}{2} J_{r_x} \dot{\phi}_r^2 + \\ &+ \frac{1}{2} J_{s_y} \dot{\theta}_s^2 + \frac{1}{2} J_{s_x} \dot{\phi}_s^2 \end{aligned} \quad (2)$$

When determining kinetic and potential energy, the curve of oscillation $v = v(x)$ of the launch pad is assumed with the function [17, 18] (Fig. 2):

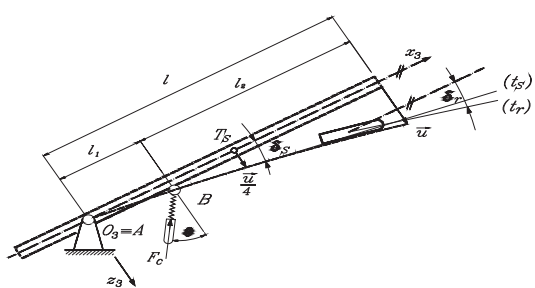


Figure 4 Angles of rotation of the rocket and centre of mass of the launching pad

$$v(x) = u \left(\frac{x}{l} \right)^2 \quad (3)$$

Potential energy of the adopted mechanical system is equal to the sum of potential energy of supports and base, centre of mass of the chassis and potential energy of deformation of the launching ramp

$$\begin{aligned} E_p &= \frac{1}{2} c_{11} (\lambda_{11} + p_{11})^2 + \frac{1}{2} c_{12} (\lambda_{12} + p_{12})^2 + \frac{1}{2} c_{21} (\lambda_{21} + p_{21})^2 + \\ &+ \frac{1}{2} c_{22} (\lambda_{22} + p_{22})^2 - g \sum m_i (z_i - z_i^0) + E_{ps} \end{aligned} \quad (4)$$

For supporting contour presented in Fig. 5:

$$\begin{aligned} p_{11} &= z_C - l_4 \varphi - l_1 \theta; p_{21} = z_C - l_4 \varphi + l_2 \theta; \\ p_{12} &= z_C + l_3 \varphi - l_1 \theta; p_{22} = z_C + l_4 \varphi + l_2 \theta \end{aligned} \quad (5)$$

Potential energy of the launch pad [19] is:
 $E_{ps} = E_{ps1} + E_{ps2} + E_{ps3}$,

where:

$$\begin{aligned} E_{ps1} &= \frac{1}{2} \int_0^l EI_{sz} \left(\frac{\partial^2 v}{\partial x^2} \right)^2 dx = k_1 \cdot u^2, \\ E_{ps2} &= \frac{1}{2} \int_0^l N(x, t) \left(\frac{\partial v}{\partial x} \right)^2 dx = k_2 u^2 + k_3 u^3, \\ E_{ps3} &= \frac{1}{2} \int_0^l f(x) v dx = k_4 u + k_5 u^2 \end{aligned} \quad (6)$$

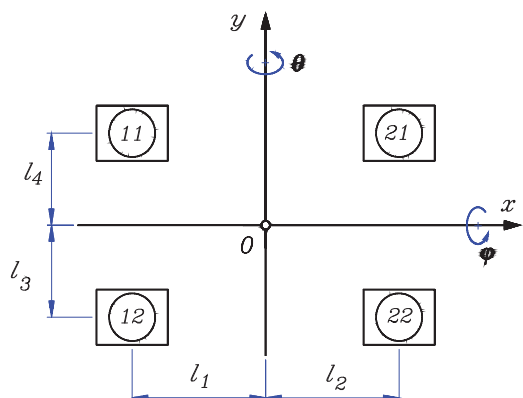


Figure 5 Supporting contour and configuration of stabilizers

Therefore, total potential energy of the launching pad is:

$$E_{ps} = E_{ps1} + E_{ps2} + E_{ps3} = k_{11} u + k_{22} u^2 + k_{33} u^3 \quad (7)$$

where the constants are respectively:
 $k_{11} = k_4$, $k_{22} = k_1 + k_2 + k_5$, $k_{33} = k_3$, $k_{22} = k_1 + k_2 + k_5$, $k_{33} = k_3$.

The expression for potential energy of the mechanical system has the final form of:

$$\begin{aligned} E_p = & \frac{1}{2} c_{11} (\lambda_{11} + p_{11})^2 + \frac{1}{2} c_{12} (\lambda_{12} + p_{12})^2 + \\ & + \frac{1}{2} c_{21} (\lambda_{21} + p_{21})^2 + \frac{1}{2} c_{22} (\lambda_{22} + p_{22})^2 - \\ & - g \sum m_i (z_i - z_i^0) + k_{11} u + k_{22} u^2 + k_{33} u^3 \end{aligned} \quad (8)$$

2.4 Coordinate Systems

According to the defined expression, generalized forces are:

$$Q_r = \sum_{i=1}^n \left(X_i \frac{\partial x_i}{\partial q_r} + Y_i \frac{\partial y_i}{\partial q_r} + Z_i \frac{\partial z_i}{\partial q_r} \right) \quad (9)$$

Generalized forces corresponding to coordinates ξ and u are:

$$Q_\xi = F_p - F_\mu - F_{ot.vaz.} \quad (10)$$

where F_p - thrust force (Fig. 6), $F_p = k \cdot t$, for $0 < t \leq t_1$, $F_p = \text{const.}$ for $t > t_1$ (when air temperature is $t = 15^\circ\text{C}$, $k = 582\,130,98 \frac{\text{N}}{\text{s}}$).

It can be considered that other generalized forces are approximately equal to zero, i.e. : $Q_u = 0$, $Q_{zC} = 0$, $Q_\phi = 0$, $Q_\theta = 0$.

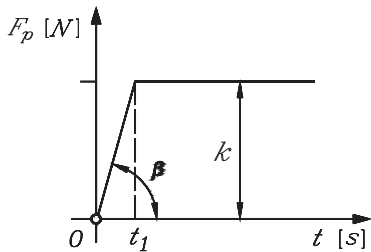


Figure 6 Change in the thrust force in the function of time

2.5 Ordinates and Velocities of Characteristic Points

Determining the radius vectors (especially ordinates) and velocity of characteristic points of such complex mechanical systems with a classical method is a very complex procedure and practically unachievable. Therefore, the paper uses a matrix method based on multiple coordinate systems, primarily set in [17] and then applied in [18].

Assuming that the position vector of any point of the system with respect to the fixed coordinate system ρ_{n0} , r_k - vector between centres of the adjacent coordinate systems O_{k-1} and O_k , and T_{k0} - matrix of cosine of angles of k -coordinate system with respect to the fixed coordinate system. Then:

$$\rho_{n0} = \mathbf{r}_{10} + \sum_{k=1}^{n-1} T_{k0} \mathbf{r}_k \quad (11)$$

Thus, the radius vectors of the centre of gravity of the mount (L), centre of gravity of the launch pad (S) and the centre of gravity of the rocket (R), respectively, are:

$$\begin{aligned} \rho_L &= \mathbf{r}_{10} + \mathbf{T}_{10} \mathbf{r}_1 + \mathbf{T}_{20} \mathbf{r}_L, \\ \rho_S &= \mathbf{r}_{10} + \mathbf{T}_{10} \mathbf{r}_1 + \mathbf{T}_{20} \mathbf{r}_2 + \mathbf{T}_{30} \mathbf{r}_{3S}, \\ \rho_R &= \mathbf{r}_{10} + \mathbf{T}_{10} \mathbf{r}_1 + \mathbf{T}_{20} \mathbf{r}_2 + \mathbf{T}_{30} \mathbf{r}_{3R} \end{aligned} \quad (12)$$

Corresponding matrices of cosine of angles are:

$$\begin{aligned} \mathbf{T}_{10} &= \begin{bmatrix} \cos\theta & \sin\varphi\sin\theta & \cos\varphi\sin\theta \\ 0 & \cos\varphi & -\sin\varphi \\ -\sin\theta & \sin\varphi\cos\theta & \cos\varphi\cos\theta \end{bmatrix}, \\ \mathbf{T}_{10} &= \begin{bmatrix} 1 & \varphi\theta & \theta \\ 0 & 1 & -\varphi \\ -\theta & \varphi & 1 \end{bmatrix} \approx \begin{bmatrix} 1 & 0 & \theta \\ 0 & 1 & -\varphi \\ -\theta & \varphi & 1 \end{bmatrix}, \\ \mathbf{T}_{20} &= \mathbf{T}_{10} \cdot \mathbf{T}_{21} = \begin{bmatrix} 1 & 0 & \theta \\ 0 & 1 & -\varphi \\ -\theta & \varphi & 1 \end{bmatrix} \cdot \begin{bmatrix} 1 & 0 & 0 \\ 0 & 1 & 0 \\ 0 & 0 & 1 \end{bmatrix} = \mathbf{T}_{10}, \\ \mathbf{T}_{30} &= \mathbf{T}_{20} \cdot \mathbf{T}_{32} = \\ &= \begin{bmatrix} \cos\psi & -\sin\psi & \theta \\ \sin\psi & \cos\psi & -\varphi \\ -\theta \cdot \cos\psi + \varphi \cdot \sin\psi & \theta \cdot \sin\psi + \varphi \cdot \cos\psi & 1 \end{bmatrix} \end{aligned} \quad (13)$$

Determining velocities by this process [17], that is increasingly used in robot dynamics, is completely formalized and comes down to derivatives of matrices, position vectors and matrix multiplications. Velocity of an arbitrary point in the system is:

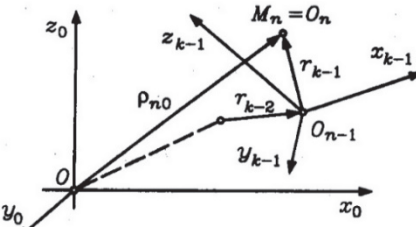


Figure 7 Radius vectors of an arbitrary point M_n position in $x_{k-1}, y_{k-1}, z_{k-1}$ coordinate system

$$\mathbf{v}_{n0} = \dot{\rho}_{n0} = \dot{\mathbf{r}}_{10} + \sum_{k=1}^{n-1} \mathbf{T}_{k0} \dot{\mathbf{r}}_k + \sum_{k=1}^{n-1} \dot{\mathbf{T}}_{k0} \mathbf{r}_k \quad (14)$$

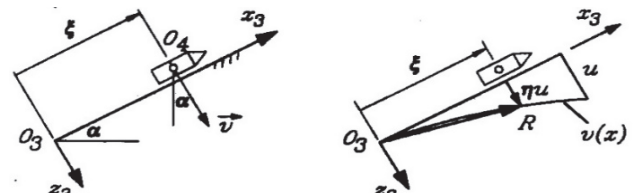


Figure 8 Deflection of the launch pad in function of the rocket on the launch pad

If velocities of the points C, L, R and S are written in a summarized form i.e. matrix form, it would simplify differential equations on the movement of a mechanical system.

- Velocity of mass centre of the chassis, point C , is:

$$v_C = \dot{z}_C \vec{k} \quad (15)$$

- Velocity of mass centre of the mount, point L :

$$v_L = \begin{bmatrix} \dot{x}_L \\ \dot{y}_L \\ \dot{z}_L \end{bmatrix} = \mathbf{H} \cdot \dot{\mathbf{q}} = \begin{bmatrix} h_{11} & h_{12} & h_{13} & h_{14} & h_{15} \\ h_{21} & h_{22} & h_{23} & h_{24} & h_{25} \\ h_{31} & h_{32} & h_{33} & h_{34} & h_{35} \end{bmatrix} \begin{bmatrix} \dot{z}_C \\ \dot{\varphi} \\ \dot{\theta} \\ \dot{\xi} \\ \dot{u} \end{bmatrix} \quad (16)$$

- Velocity of mass centre of the rocket (point R) and velocity of mass centre of the shaft (point S) are:

$$v_R = \begin{bmatrix} \dot{x}_R \\ \dot{y}_R \\ \dot{z}_R \end{bmatrix} = \mathbf{F} \cdot \dot{\mathbf{q}}, v_S = \begin{bmatrix} \dot{x}_S \\ \dot{y}_S \\ \dot{z}_S \end{bmatrix} = \mathbf{G} \cdot \dot{\mathbf{q}} \quad (17)$$

2.6 Mathematical Model-Differential Equations of the Motion of the Mechanical System

In order to derive differential equations of the motion, the Lagrange's equations of the second kind are used:

$$\frac{d}{dt} \left(\frac{\partial E_k}{\partial \dot{q}_r} \right) - \frac{\partial E_k}{\partial q_r} + \frac{\partial E_p}{\partial q_r} = Q_r^N, \quad (r=1, 2, \dots, 5), \quad (18)$$

$q_r = z_C, \varphi, \theta, \xi, u$

Obtained mathematical model represents a system of five nonlinear, nonhomogeneous differential equations of second order. The given system of differential equations is similar to Lyapunov's system and it is solved by separating small parameters in the form of a row (Selmic, 1979). However, the aforementioned system is solved faster and simpler by using discrete numerical methods, which are quite efficiently done on computers. Runge-Kutta method is recommended for solving these systems of differential equations. Due to this, systems of differential equations should be written in the form of a matrix:

$$\mathbf{A} \cdot \ddot{\mathbf{q}} + \mathbf{B} \cdot \dot{\mathbf{q}} + \mathbf{C} \cdot \mathbf{q} = \mathbf{D} \quad (19)$$

Software package MATLAB enables solving nonlinear differential equations. Due to the application of MATLAB it was necessary to write differential equations of motion in the form of a matrix, as follows:

$$\mathbf{A} \cdot \ddot{\mathbf{q}} = -(\mathbf{B} \cdot \dot{\mathbf{q}} + \mathbf{C} \cdot \mathbf{q} + \mathbf{D}), \text{ i.e. } \mathbf{A} \cdot \ddot{\mathbf{q}} = -\mathbf{S} \quad (20)$$

where the following is obtained:

$$\ddot{\mathbf{q}} = -\mathbf{A}^{-1} \cdot \mathbf{S}, \text{ i.e., } \begin{bmatrix} \ddot{z}_C \\ \ddot{\varphi} \\ \ddot{\theta} \\ \ddot{\xi} \\ \ddot{u} \end{bmatrix} = -\mathbf{A}^{-1} \cdot \begin{bmatrix} S_{11} \\ S_{21} \\ S_{31} \\ S_{41} \\ S_{51} \end{bmatrix} \quad (21)$$

Expressions for accelerations and velocities prepared in such a way can be solved by the software through the previous replacement of variables in the following way:

$$x_1 = z_C, x_2 = \dot{z}_C, x_3 = \varphi, x_4 = \dot{\varphi}, x_5 = \theta, x_6 = \dot{\theta}, \\ x_7 = \xi, x_8 = \dot{\xi}, x_9 = u, x_{10} = \dot{u}$$

Thus the system of differential equations has the following form:

$$\mathbf{A}(z_C, \varphi, \theta, \xi, u) \cdot \begin{bmatrix} \ddot{z}_C \\ \ddot{\varphi} \\ \ddot{\theta} \\ \ddot{\xi} \\ \ddot{u} \end{bmatrix} = \mathbf{S}(z_C, \varphi, \theta, \xi, u, \dot{z}_C, \dot{\varphi}, \dot{\theta}, \dot{\xi}, \dot{u}) \quad (22)$$

and it is transformed to a system of 10 differential equations of the first order, suitable for numerical solving through the software package MATLAB. A numerical analysis of this problem was performed for a concrete construction.

3 RESULTS ANALYSIS

The numerical analysis was performed in the case when the hydro-cylinder is replaced with resistance force linearly proportionate to the first degree of velocity of point B (Fig. 2), i.e. the force in hydro-cylinder is:

$$F_c = F_{c1} + F_{c3} = \frac{\pi}{2} (D^2 - d^2) + b_{cil} \dot{u} (l_1) \cos \theta \quad (23)$$

Graphic overview of characteristic parameters is given in Fig. 9 to Fig. 12.

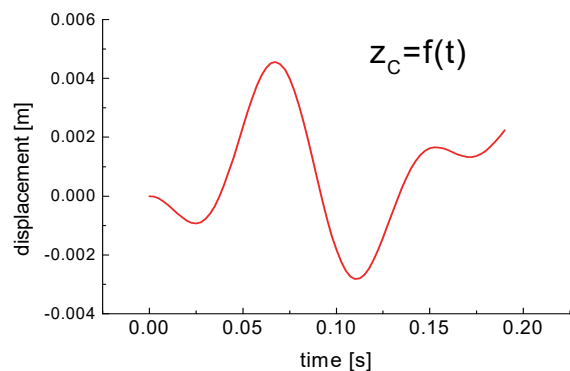


Figure 9 Displacement of the system's center of mass

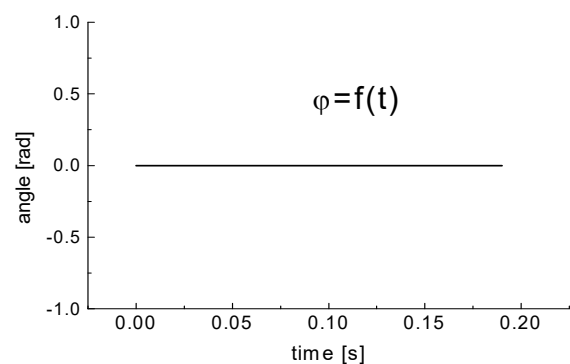


Figure 10 Angle of rotation around the longitudinal axis

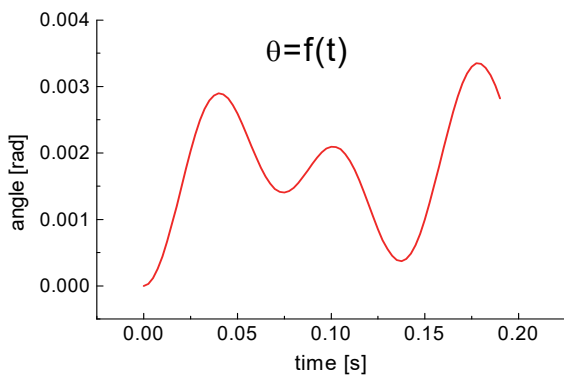


Figure 11 Angle of rotation around transversal axis

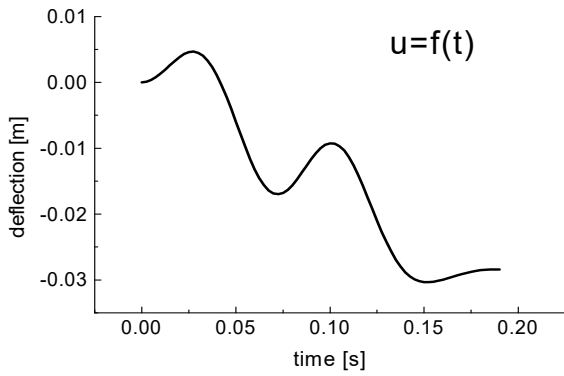


Figure 12 Deflection of the top of the ramp

Based on the input data and obtained diagrams it can be concluded that: 1) displacement of mass centre of the chassis occurs in the limits of up to 0,009 m (Fig. 9), 2) rotation around x -axis does not exist because all masses are on that axis (Fig. 10), 3) rotation around y -axis exists to thrust force and momentum during movement of the rocket on the launch pad, and is performed to harmonic function (Fig. 11), 4) deflection of the launch pad is the biggest at the end of the launch pad and it is of a nonlinear character and amounts to 0,03 m (Fig. 12).

From the attached diagrams, especially Fig. 12 it is visible that the hydro-cylinder needs to be approximated only by damping high stiffness. Curve of deflection authentically follows the curve obtained by measuring. An analysis of influential parameters was performed for the adopted mechanical model. Graphic overview of characteristic parameters is given in Fig. 13 to Fig. 16.

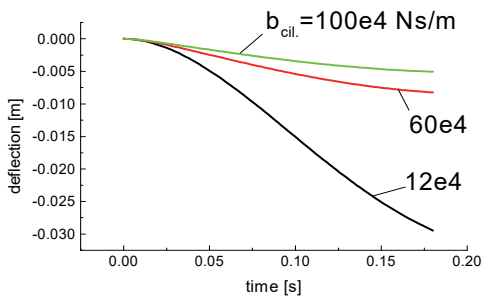


Figure 13 Deflection depending on viscous friction of the hydro-cylinder

Based on the variations of the given parameters it can be concluded that: 1) by reducing the values of coefficients of viscous friction of a hydro-cylinder, deflection of the launch pad's top increases (Fig. 13), 2) depending on the required velocity of deflection of the launch top of the ramp, it is possible to pick the value of the coefficient of

viscous friction of a hydro-cylinder (Fig. 14), 3) deflection of the launch pad reduces with reduction of rocket's mass almost linearly (Fig.15, Fig. 16).

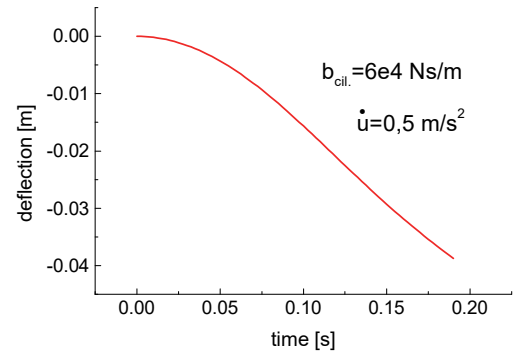


Figure 14 Deflection velocity of the ramp

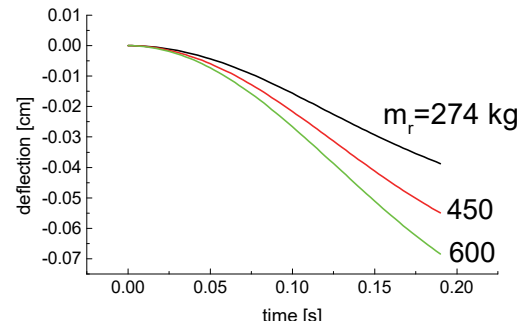


Figure 15 Deflection of the ramp in function of rocket motion time of different masses

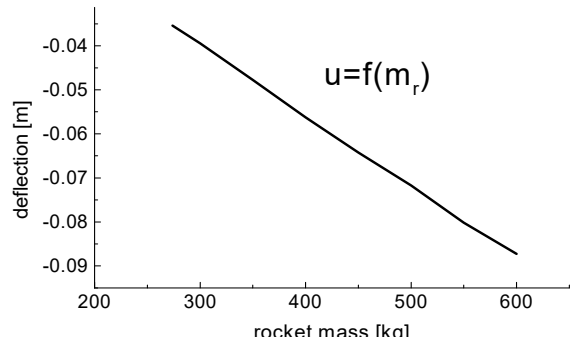


Figure 16 Deflection depending on rocket mass

4 MEASURING AND STATISTICAL PROCESSING OF RESULTS

Measurements were performed on a self-propelled launcher while launching a rocket. Single and burst fire launches were observed. A point was observed, firstly the left and second time the right (Fig. 2) part of the launch pad and its motion in the vertical plane (deflection of the top). In case when the measuring point was right part of the top of launch pad, three shots were measured (Fig. 18). In case when the measuring point was left part of the top of the ramp, four shots were measured (Fig. 19). In case when three rockets were fired at once, two measurements were taken (Fig. 20). During the aforementioned measurements, the launch pad was directed at the material axis of the system with a direction x_0 -axis, i.e. angle of azimuth was $\psi = 0$ (Fig. 3). Three measurements (Fig. 21) were performed for an angle of azimuth $\psi = 20^\circ$. In all cases the angle of inclination of the launch pad in a vertical plane was $\alpha = 45^\circ$ and the observed deflection of

the top of the ramp was in function of the time that the rocket moved on the ramp. When performing experiments according to this one in Fig. 17, the following equipment was used: 1) Camera 1: stationary camera; 2) Camera 2: manual tracking of the rocket (from hand); 3) radar for measuring speed; 4) observation equipment.

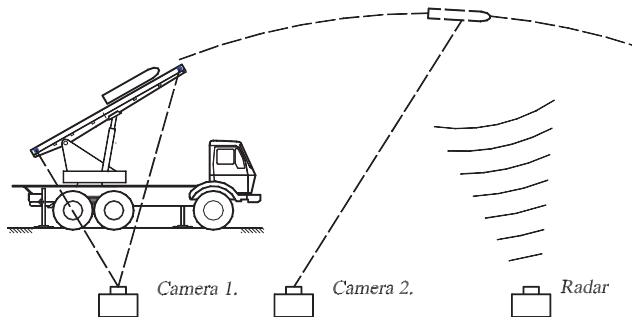


Figure 17 Position of the measuring equipment during the experiment

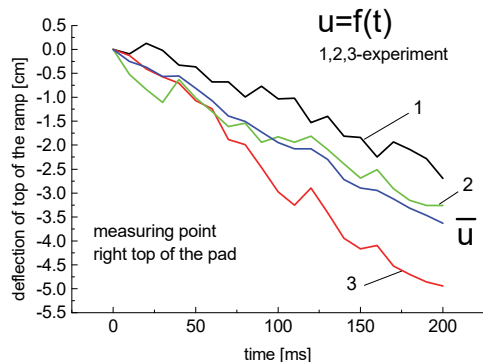


Figure 18 Deflection of the ramp during the experiment -measuring point, right at the top of the pad

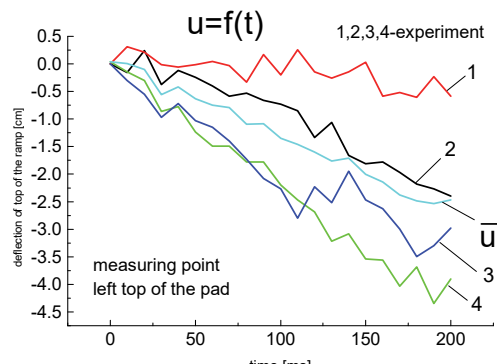


Figure 19 Deflection of the ramp during experiment -measuring point, left at the top of the pad

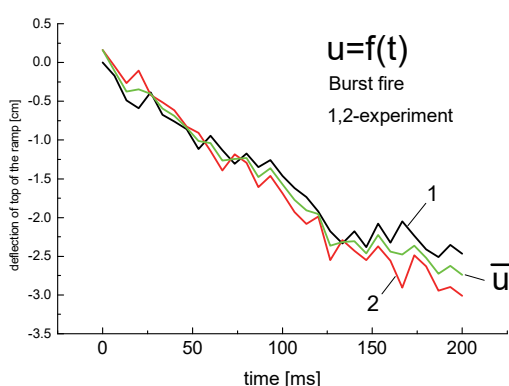


Figure 20 Deflection of the ramp during experiment - burst fire

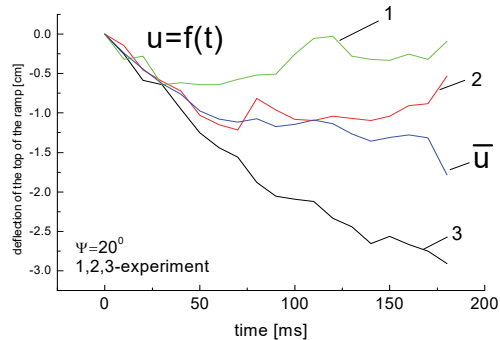


Figure 21 Deflection of the ramp during the experiment - ramp rotated for $\psi = 20^\circ$ from the longitudinal axis to the left

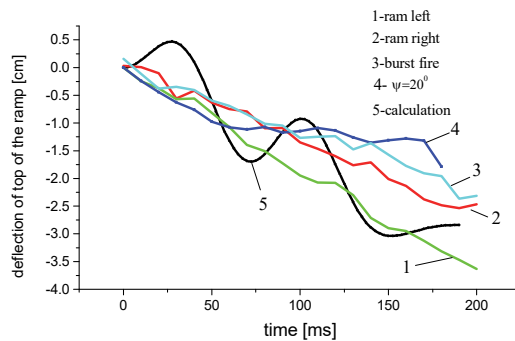


Figure 22 Comparing the deflection curves of the top of the launch pad obtained by experiment and calculation

Based on the data input and obtained diagrams it can be concluded: (1) A point at the top of the launch pad on the right was observed. Three shots were taken (curves 1, 2, 3). The smallest square deviation (SSD) from the mean value or standard deviation was $\sigma = 2,19$, which means that 66% of experiments were taken into consideration, and in the case of $2\sigma = 4,38$; 95% of experiments were included. (curve \bar{u} , Fig. 18); (2) A point at the top of the launch pad on the left was observed. Four shots were taken (curves 1, 2, 3, 4). The SSD from the mean value or standard deviation was $\sigma = 2,03$, which means that 66% of experiments were taken into consideration, and in case $2\sigma = 4,06$; 95% of experiments were included. (curve \bar{u} , Fig. 19); (3) A point at the top of the launch pad was observed. Two shots were taken at the same time (burst fire, curves 1 and 2). The SSD from the mean value or standard deviation was $\sigma = 1,61$, which means that 66% of experiments were taken into consideration, and in the case of $2\sigma = 3,22$; 95% of experiments were included. (curve \bar{u} , Fig. 20); (4) A point at the top of the launch pad was observed with rotated launch pad from the longitudinal axis to the left for 20° . Three shots were taken (curves 1, 2, 3). The SSD deviation from the mean value or standard deviation is $\sigma = 1,2$, which means that 66% of the experiments were taken into consideration, and in the case of $2\sigma = 2,4$; 95% of the experiments were included. (curve \bar{u} , Fig. 21); (5) All four curves were compared with the calculation curve. It is evident that the calculation provides satisfying results, thus it is not necessary to perform expensive experiments (Fig. 22). Deflection curves of the top of the ramp obtained by measuring (curves 1, 2, 3, 4, Fig. 22) show increase of deflection over time, i.e. while the rocket gets closer to the top of the launch pad. Those curves have an accidental

character and their change can be characterized as irregular harmonic change of small amplitudes. Deflection curve of the top of the pad obtained by numerical interpretation of an adopted mechanical-mathematical model (curve 5) is relatively agreed to the curves obtained measurements (curves 1, 2, 3, 4). Clearly expressed oscillatory character of curve 5, relative to the large oscillatory amplitudes is the consequence of elasticity of the pad and support in hydro-cylinder which are taken in the considered model.

5 CONCLUSION

Influence of each construction and exploitation parameter on the behaviour of the rocket system can be determined by mathematical modelling and simulation on a computer in the design or modification phase. This is of great importance because it rationalizes the entire project. Since a solution of the mathematical model can be used when analysing the influence of concrete construction parameters on certain properties of the rocket system, from that part of the research, the following conclusions can be made: (1) It is known that angular velocities around characteristic axis (transversal and longitudinal axis) have an important influence on the position of hits. The smallest spread on the target is obtained by positioning the launch pad in a position that causes the smallest values of the mentioned angular velocities. Simulation can find parameters of a most favourable position of the system, considering accuracy and precision. (2) Declination angle of a launch pad has a significant influence on the flow of the oscillatory process of a rocket system. It influences the deflection but in a smaller degree than stiffness of the support. This paper gives a comprehensive approach to the problem of oscillatory motion of the rocket system. Basic assumption of the dynamic model is that, after a rocket is launched from the launch ramp, rocket system performs muffled oscillations. Disturbances during rocket's start represent initial conditions for oscillations. Rocket system requirements regarding weight and range require more complete calculation methods for the entire construction, especially a more precise determination of dynamic loads. The method presented in this paper enables determining dynamic loads of mechanical stabilizers (supports) taking into consideration elasticity of the base. It is possible to determine dynamic loads of the launch pad, depending on parameters of the support and stiffness of the base.

Abbreviations and symbols:

Z_C - Vertical displacement of the centre of mass (point $C \equiv O_0$) of the lower part (of a chassis),
 φ - Rotation around the longitudinal main central axis of inertia O_1x_1 of the lower part (of a chassis),
 θ - Rotation around the transversal main central axis of inertia O_1y_1 of the lower part (of a chassis),
 u - Deformation of the top of the launch pad in vertical plane, perpendicular to the longitudinal axis of the launch pad,
 ξ - Movement of the rocket on the launch pad,
 $x_0y_0z_0$ - Fixed coordinate system with centre O_0 in point

C adopted for the whole system (chassis, platform, launch pad, rocket). Axis Ox_0 coincides with the longitudinal and axis Oy_0 with transversal main central axis of inertia of the lower part in an equilibrium position and axis Oz_0 is directed vertically downward,

$x_1y_1z_1$ - Mobile coordinate system connected to the chassis with the centre O_1 in the point C (chassis' centre of mass). Ox_1 axis coincides with the longitudinal and Oy_1 axis with the transversal central axis of inertia in an equilibrium and Oz_1 axis is directed vertically downwards,

$x_2y_2z_2$ - Mobile coordinate system adopted for a mount and a launch pad with the centre in point O_2 which intersects the longitudinal axis of the mount and horizontal plane which passes through the joint of the launching ramp,

$x_3y_3z_3$ - Mobile coordinate system with the centre O_3 in the joint of the launch pad, directed axis x_3 at the top of the launch pad, y_3 perpendicular to the launch pad and z_3 axis is directed perpendicularly to the $O_3x_3y_3$ plane,

E_{k1} - Kinetic energy of the chassis and related components,

E_{k2} - Kinetic energy of the rocket and the launch pad,

m_1 - Mass of the chassis and related components,

\dot{Z}_C - Velocity of mass centre of the chassis,

x - Coordinate on longitudinal central axis of the ramp,

v_L - Velocity of the mount's centre of mass,

l - Length of the ramp from support-joint to the top of the ramp,

J_{1x} - Moment of inertia of the chassis for longitudinal O_1x_1 axis, which passes through the mass centre of the chassis O_1 ,

$\dot{\varphi}$ - Angular velocity of the chassis around its longitudinal axis of inertia O_1y_1 ,

$\dot{\theta}$ - Angular velocity of the chassis around its transversal axis of inertia O_1x_1 ,

J_{1y} - Moment of inertia of chassis for transversal y_1 - axis, longitudinal O_1x_1 axis, which passes through the mass centre of the chassis O_1 ,
 m_L - Mass of the mount,

J_{Lx_2} - Moment of inertia of the mount for longitudinal x - axis, longitudinal O_1x_1 axis, which passes through the mass centre of the chassis O_1 ,

J_{Ly_2} - Moment of inertia of the mount for transversal y - axis, longitudinal O_1x_1 axis, which passes through the mass centre of the chassis O_1 ,

$$J_{Lx_2} = J_{2x}^* \cos^2 \psi + J_{2y}^* \sin^2 \psi - J_{2xy}^* \sin 2\psi ,$$

$$J_{Ly_2} = J_{2x}^* \sin^2 \psi + J_{2y}^* \cos^2 \psi + J_{2xy}^* \sin 2\psi ,$$

J_{2x}^*, J_{2y}^* - Moments of inertia of upper elements for corresponding axis in position shown in Fig. 1,

J_{rx}, J_{ry} - Moments of inertia of the rocket for corresponding axis of the chassis,

J_{sx}, J_{sy} - Moments of inertia of the shaft for corresponding axis of the chassis,

m_r - Mass of the rocket,

v_r - Velocity of the rocket,
 $\dot{\delta}_r$ - Angular velocity of the rocket around its lateral central axis O_4y ,
 $\dot{\delta}_s$ - Angular velocity of the launch pad around lateral central axis of the ramp,
 m_s - Mass of the launch pad,
 v_s - Displacement velocity of the mass centre of the launch pad due to elastic support and deformation of the launch pad,
 $c_{j,k}$ - Reduced stiffness of the base and support (stabilizers),
 $p_{j,k}$ - Reduced dynamic deformation of the base and support (stabilizers),
 $\lambda_{j,k}$ - Corresponding static deformations,
 Z_i, Z_i^0 - Current and initial ordinates of the centre of mass of system elements,
 E_{ps1} - Potential energy of elastic deformation of the launch pad due to bending (not taking into consideration shearing),
 E - Modulus of elasticity of ramp material,
 I_{S_y} - Moment of inertia of surface of the cross-section of the launch pad for axis $y - y_i$,
 k_1 - Constant that depends on launch pad parameters,
 E_{ps2} - Potential energy of pressure - stretching of the launch pad due to action of resulting axial force $N(x, t)$: from continual load of the launch pad, rocket load, deformation of a hydraulic cylinder and friction force,
 k_2, k_3 - Constants that depend on shaft and rocket mass, friction coefficient, stiffness of hydro-cylinder and geometry of the launch pad and hydro-cylinder,
 E_{ps3} - Potential energy of the launch pad due to resulting transversal force from rocket load, continual load of the launch pad and force in the hydraulic cylinder,
 Q_ξ - Generalized force corresponding to coordinate ξ ,
 Q_u, Q_{z_C} - Generalized force corresponding to coordinate u ,
 Q_φ, Q_θ - Generalized force corresponding to coordinate φ and θ , respectively,
 b_L, r_{3S}, r_{3R} - Radius vectors of the gravity centre of the mount, ramp and rocket in corresponding coordinate,
 \dot{r}_k - Local derivative of the vector,
 F_p - Thrust force of the rocket engine,
 F_μ - Friction force of the rocket to the Launchpad,
 $F_{ot.vaz.}$ - Air resistance force during motion of the rocket on the launch pad,
 ρ_{n0}, r_k - Vector between centres of adjacent coordinate systems O_{k-1} and O_k ,
 T_{k0} - Matrix of cosine of angles of k - coordinate system with respect to fixed coordinate system,
 H, F, G - Constants or functions of defined coordinates or velocities,
 A, B, C, D - Corresponding matrices are functions of generalized coordinates and velocities,
 A - Inertia matrix,
 B - Damping matrix,

C - Rigidity matrix,
 D - Excitation matrix,
 D, d, θ - Geometric cylinder parameters,
 b_{cil} - Damping coefficient in the cylinder,
 α - Angle of inclination of the launch pad,
 ψ - Angle of azimuth of the launch pad.

6 REFERENCES

- [1] Svetlickij, V. A. (1986). Start dynamics of flying devices (in Russian), *Nauka*, Moscow.
- [2] Isik, C., Ider, S. K., & Acar, B. (2014). Modeling and verification of a missile launcher system. *Proc IMechE Part K: JMultibody Dynamics*, 228(1), 100-107. <https://doi.org/10.1177/1464419313485942>
- [3] Dziopa, Z., Buda, P., Nyckowski, M., & Pawlikowski, R. (2015). Dynamics of an unguided missiles launcher. *Journal of Theoretical and Applied Mechanics*. <https://doi.org/10.15632/jtam-pl.53.1.69>
- [4] Xinlin, W., Jiang, Y., Zeng, W., & Pan, X. (2016). The coupling effects of the missile launcher and the ground in vehicle-mounted missile erecting. *Advances in Mechanical Engineering*, 8(7), 1-12. <https://doi.org/10.1177/1687814016656106>
- [5] Pamfioryl, S. & Cristian, E. M. (2013). Numerical Research on The Stability of Launching Devices During Firing. *Defence Technology*, 9, 242-248. <https://doi.org/10.1016/j.dt.2013.12.005>
- [6] Šomoiaig, P., Safta, D., & Moldoveanu, E. C. (2008). Particularity of the Rocket Movement upon the Launcher under the Disturbance Factors Action which Appear During the Firing. *Proceedings of the World Congress on Engineering 2008 II, WCE 2008*.
- [7] Zivanic, D., Milosevic, M., Pajcini, M., Bugaric, U., Petrovic, D., & Petrovic, Z. (2011). Defining the Elasticity Elimination Mechanism of Multiple Rocket Launcher Vehicle. *FME Transactions*, 39, 171-175.
- [8] Zhan, H. Z., Rui, T. X., Rong, B., Yang, F. F., & Wang, P. G. (2011). Design of active vibration control for launcher of multiple launch rocket system. *Proc. IMechE*, 225. <https://doi.org/10.1177/1464419311406808>
- [9] Wang, X., Rui, X., Yang, F., & Zhou, Q. (2018). Launch Dynamics Modeling and Simulation of Vehicular Missile System. *ARC Aerospace Research Central*.
- [10] Li, B. & Rui, X. (2018). Vibration control of uncertain multiple launch rocket system using radial basis function neural network. *Mechanical Systems and Signal Processing*, 98, 702-721. <https://doi.org/10.1016/j.ymssp.2017.05.036>
- [11] Li, B., Rui, X., & Zhou, Q. (2018). Study on simulation and experiment of control for multiple launch rocket system by computed torque method. *Nonlinear Dynamics*, 91(3), 1639-1652. <https://doi.org/10.1007/s11071-017-3970-7>
- [12] Wang, G., Rui, X., & Tang, W. (2017). Active vibration control design method based on transfer matrix method for multibody systems. *Journal of Engineering Mechanics*, 143, 6. [https://doi.org/10.1061/\(ASCE\)EM.1943-7889.0001236](https://doi.org/10.1061/(ASCE)EM.1943-7889.0001236)
- [13] Dernlugkam, N. & Chodsirisak, R. (2017). Modeling and analysis of a prototype of multiple launch rocket system using Matlab Simulink. *Proceedings of 78th IASTEM International Conference*, Singapore, 53-57:
- [14] Li, B., Rui, X., Zhou, Q., Zhang, J., & Gu, L. (2018). Modeling, Simulation and Experiment of Multibody System Launch Dynamics for Multiple Launch Rocket System, *14th International Conference on Multibody Systems, Nonlinear Dynamics, and Control*, 6. Quebec City. <https://doi.org/10.1115/DETC2018-85790>
- [15] Yang, H., Fu, X., Zhan, Z., & Xin, W. (2019). Parameterization dynamics visual design platform for

- missile launching system. *Advances in Mechanical Engineering*. <https://doi.org/10.1177/1687814019827129>
- [16] Rui, X., Wang, X., Zhou, Q., & Zhang, J. (2019). Transfer matrix method for multibody systems (Rui method) and its applications. *SCIENCE CHINA Technological Sciences*, 62(5), 712-720. <https://doi.org/10.1007/s11431-018-9425-x>
- [17] Selmic, R. R. (1979). *Contribution to dynamic loads research of carriage construction of the auto crane with special chassis, hydro driver and telescope cantilever*. Ph.D. Thesis, University of Belgrade, Faculty of Mechanical Engineering.
- [18] Djurkovic, P. V. (2001). Contribution to optimal parameters ascertainment for launching aircraft. Ph.D. Thesis, Military academy of the National Army of Yugoslavia, Belgrade.
- [19] Raskovic, D. (1957). *Oscillation theory*. Naučna knjiga, Belgrade.
- [20] Jolović, I. & Bobera, D. (2019). Analysis of the project manager's role in the research and development projects. *Oditor*, 5(3), 38-52. <https://doi.org/10.5937/Oditor1903038J>
- [21] Rui, X., Wang, G., & Zhang, J. (2019). Transfer Matrix Method for Multibody Systems-Theory and Applications, Google Books. *John Wiley & Sons Singapore Pte. Ltd.*

Contact information:

Dragoljub VUJIC, PhD, Full Professor
(Corresponding author)
Military Technical Institute,
1 Ratka Resanovica Str.,
11000 Belgrade, Serbia
E-mail: vujicd@eunet.rs

Vlado DJURKOVIC, PhD, Full Professor
University of Defence,
Military Academy,
33 Pavla Jurisica Sturma Str.,
11000 Belgrade, Serbia
E-mail: djurkovic.vlado@gmail.com

Nikola MILENKOVIĆ, PhD, Assistant Professor
School of management and economic studies,
52 Karadjordjeva Str.,
34000 Kragujevac, Serbia
E-mail: milenkovic.nikola989@gmail.com

Slavisa TRAJKOVIC, PhD, Full Professor
Faculty of Economics, University of Pristina,
156 Kolasinska Str.,
38220 Kosovska Mitrovica, Serbia
E-mail: slavisa.trajkovic@pr.ac.rs